Joint Radar-Communication Waveform Designs Using Signals from Multiplexed Users

Ning Cao, Yunfei Chen, *Senior Member, IEEE*, Xueyun Gu, Wei Feng, *Senior Member, IEEE*

***Abstract*— Joint radar-communication designs are exploited in applications where radar and communications systems share the same frequency band or when both radar sensing and information communication functions are required in the same system. Finding a waveform that is suitable for both radar and communication is challenging due to the difference between radar and communication operations. In this paper, we propose a new method of designing dual-functional waveforms for both radar and communication using signals from multiplexed communications users. Specifically, signals from different communications users multiplexed in the time, code or frequency domains across different data bits are linearly combined to generate an overall radar waveform. Three typical radar waveforms are considered. The coefficients of the linear combination are optimized to minimize the mean squared error with or without a constraint on the signal-to-noise ratio (SNR) for the communications signals. Numerical results show that the optimization without SNR constraint can almost perfectly approximate the radar waveform in all the cases considered, giving good dual-functional waveforms for both radar and communication. Also, among different multiplexing techniques, time division multiple access is the best option to approximate the radar waveform, followed by code division multiple access and orthogonal frequency division multiple access.**

***Index Terms*— Code division multiple access, joint radar-communications, orthogonal frequency division multiple access, time division multiple access, waveform designs.**

I. Introduction

Historically radar and communications systems are developed separately due to their distinct functions. In recent years, the two systems have started to merge with each other for two main reasons [1]. Firstly, the "spectrum scarcity" problem in communications is becoming more serious, making it imperative for the communications systems to utilize as many available frequency bands in the radio spectrum as possible, including the radar bands that are being opened for shared access [2]. Hence, interference between radar and communications is inevitable to make joint radar-communication designs desirable [3]. Secondly, future emerging applications require both information communication and radar sensing functions in the same system, such as autonomous driving and asset tracking [4]. This necessitates joint designs for integrated radar-communication functions.

Although radar and communications systems adopt similar statistical signal processing techniques [5], they still have considerable difference. These different characteristics bring challenges to joint radar-communication designs. One such challenge is the waveform design, where radar and communication functions have different requirements for a "good" waveform, while a single waveform has to be used for both radar and communication functions in a unified radar-communication system. Consequently, a lot of researches have been conducted to find dual-functional waveforms [6]. These dual-functional waveforms, including the one to be proposed, can be used in the application discussed in [4]. They can also be used in vehicular communications to communicate data while detecting obstacles [7], in low probability-of-interception communications to increase the data security by hiding communications data in the radar pulse [8], and in radio frequency identification to communicate information while localizing tags [9]. More application scenarios are in [1].

A widely used approach is to embed the communication symbols into the radar waveform. For example, in [10], the antenna array was divided into several subarrays, each of which transmitted an orthogonal radar waveform. The communications symbols were embedded in the magnitude or phase difference of the waveform pairs. Similarly, in [11], the communications symbols were embedded in the radar waveform by controlling different spread sequences as orthogonal waveforms for radar, and the receiver decoded the transmitted information by determining which sequence has been transmitted. In [12] and [13], the communications symbols were embedded in the radar waveform by modulating the phase or amplitude of the linear frequency modulation (LFM) waveform for radar so that the radar waveform acted as a carrier for communications. In [14], the communications symbols were embedded in the radar waveform by re-modulating the incident radar signal. Another widely used method is waveform diversity. For example, in [15] and [16], the radar signal was transmitted over the main lobe of an antenna array, while the communications symbols were transmitted over the side lobes of the same array. In [17], radar and communication were combined by modulating the same carrier, where the frequency of the carrier was modulated by LFM for radar and the phase of the carrier was modulated by continuous phase modulation (CPM) for communications, simultaneously. In [18], they were combined by modulating

The work of Ning Cao was supported in part by the National Natural Science Foundation of China (41830110). The work of Wei Feng was supported in part by the National Natural Science Foundation of China (61941104, 61922049, 61701457, 61771286) and the Beijing Innovation Center for Future Chip. The corresponding author is Wei Feng.

Ning Cao is with the College of Computer and Information, Hohai University, Nanjing, 211100, China (e-mail: caoning@vip.163.com).

Yunfei Chen and Xueyun Gu are with the School of Engineering, University of Warwick, Coventry, CV4 7AL, UK (e-mail: Yunfei.Chen, Xueyun.Gu@warwick.ac.uk).

Wei Feng is with the Beijing National Research Center for Information Science and Technology, Department of Electronic Engineering, Tsinghua University, Beijing 100084, China. He is also with the Peng Cheng Laboratory, Shenzhen 518055, China (e-mail: fengwei@tsinghua.edu.cn).

the phase of the same carrier, where one phase term represents radar and another phase term represents communications. In [19], an orthogonal frequency division multiplexing (OFDM) signal was used for communications but its parameters were tuned to make it suitable for radar applications. In the radar research alone, OFDM waveform design is an interesting topic [21], [22]. Other works considered the optimization of radar waveforms to minimize its impact on the co-existing communications systems [20]. More interesting discussions on dual-functional waveform designs can be found in [23].

All the aforementioned works have given very useful guidance on dual-functional waveform designs. However, most of these works have used the signal from only one communications user in their designs. On the other hand, in many communications systems, the base station often serves more than one user in the downlink. For such systems adopting multiple antennas, references [24] - [26] studied different beamforming schemes to explore the spatial orthogonality of users for dual-functional waveforms. If these systems use single antennas or multiple antennas without beamforming, the spatial orthogonality cannot be used but users are still multiplexed using either time division multiple access (TDMA), code division multiple access (CDMA), or orthogonal frequency division multiple access (OFDMA) and hence, the time, code or frequency orthogonality of multiple multiplexed users can be exploited for dual-functional waveform designs. One such approach is to combine the signals from multiple communications users in different bit intervals to approximate the radar waveform so that the radar receiver can use the overall approximated waveform for target detection while the communications receivers can separate their signals from the overall waveform using orthogonal functions in the time, code, and frequency domains for information decoding.

The purpose of this work is to study the problem of approximating a radar pulse using signals from multiplexed communications users over different bit intervals to design a dual-functional waveform for both radar and communication. Specifically, the signals from different TDMA, CDMA or OFDMA users are linearly combined. The coefficients of the linear combination are derived by minimizing the mean squared error. Both the unconstrained minimization to emphasize the approximation accuracy for radar function and the constrained minimization to avoid degrading quality of service for communications due to linear combination are considered. Numerical results are presented to show that TDMA has the highest accuracy, followed by CDMA and OFDMA. Also, TDMA and CDMA can approximate all three commonly used radar pulses reasonably well. The main contributions of this work can be summarized as follows.

- Most previous works on dual-functional waveform designs mainly use the communications signal from one user in one bit interval, while our work uses communications signals from multiple users in multiple bit intervals. When multiple users are considered, [24] - [26] explore the orthogonality in the space domain, while our work explores the orthogonality in the time, code or frequency domains.
- Previous works implement dual-functional waveforms by either embedding the communication symbol into the radar waveform, beamforming an antenna array to generate different beam patterns for radar and communications, or modulating the same carrier with both radar and communications waveforms. Our work proposes a new method of approximating the radar waveform using multiple communications signals multiplexed in time, code and frequency so that the overall waveform can be used for radar function, while its individual parts can be used for communications.
- The optimum combinations of communications signals and the optimum approximations are derived and compared with the exact radar pulses.
- The proposed approximations have very high accuracy and thus, they can offer an efficient joint radar-communication design.

The rest of the paper is organized as follows. In Section II, the system model of the work will be introduced. Section III will derive the optimum combination of communications signals to approximate the radar pulses. In Section IV, numerical results will be provided to verify the accuracy of the approximation. Finally, in Section V, concluding remarks will be made.

II. System Model

Consider a joint radar-communication system with one central controller or base station. The base station acts as a mono-static radar station that transmits a radar pulse and receives the returned radar pulse for target detection. Although the mono-static radar is assumed in the following, the results can be applied to bi-static and multi-static radars too, as long as the radar transmitter is collocated with the communications transmitter and multiple signals are available to enable the linear combination. To integrate the communication function into the radar function, it also acts as an access point to serve K communications users by transmitting signals in the downlink to receivers at K communications users, $K > 1$. Thus, the signals for the K communications users must be combined with or embedded in the radar pulse in the joint radar-communication setting. Assume that the radar pulse has a duration of T with a bandwidth of B. Also, assume that each bit of the communications signals occupies a time interval of T_b. Since the radar pulse repetition frequency is normally much smaller than the data rate in communications systems, we assume that $T = T_b * L$, or there are L bits of communications signals within each radar pulse, $L > 1$.

For the radar pulse, one widely used waveform is the LFM pulse. The baseband representation of a LFM pulse is given by [27]

$$r(t) = e^{j\pi \frac{B}{T} t^2}, 0 < t < T. \tag{1}$$

Also, the Gaussian pulse and Barker sequence are frequently used in radar applications. The Gaussian pulse is given by [28]

$$r(t) = e^{-\frac{B}{T}(t-\frac{T}{2})^2}, 0 < t < T, \tag{2}$$

which is centered at $t = \frac{T}{2}$. The Barker sequence is given by

[29]

$$r(t) = \sum_{m=0}^{M-1} b_m a(t - mH), 0 < t < T \tag{3}$$

where M is the length of the Barker code, b_m is the value of the Barker code, $H = \frac{T}{M}$ is the duration of each code, and $a(t) = \epsilon(t) - \epsilon(t - H)$ with $\epsilon(t)$ being the unit step function so that $\epsilon(t) = 1$ when $t > 0$ and $\epsilon(t) = 0$ when $t < 0$.

For the multiple communications users, to avoid mutual interference so that only the desired signal is recovered at the designated communications receiver, their signals are usually transmitted over orthogonal resource blocks using multiplexing. One widely used multiplexing method is TDMA, where signals for different communications users are transmitted in different time slots. For TDMA, the communication pulse in the l-th bit of the k-th user is given by

$$g_{kl}(t) = \epsilon\left(t - \left(l + \frac{k-1}{K}\right)T_b\right) - \epsilon\left(t - \left(l + \frac{k}{K}\right)T_b\right) \tag{4}$$

where $l = 0, 1, \cdots, L-1$, $k = 1, 2, \cdots, K$ and $\epsilon(t)$ is the unit step function defined as before. Effectively, each bit interval of T_b has been divided into K time slots, where the signal for the k-th user is transmitted in the k-th time slot during each bit. These time slots are orthogonal with each other.

Alternatively, CDMA can be used. In this case, the communication pulse in the l-th bit of the k-th user is given by

$$\begin{aligned} g_{kl}(t) &= \sum_{i=1}^{I} d_{ki}\left[\epsilon\left(t - \left(l + \frac{i-1}{I}\right)T_b\right)\right. \\ &\quad \left. -\epsilon\left(t - \left(l + \frac{i}{I}\right)T_b\right)\right] \end{aligned} \tag{5}$$

where d_{ki} is the spreading code of the i-th chip for the k-th user, I is the processing gain or the length of the spreading sequence, l and $\epsilon(t)$ are defined as before. In this case, the spreading sequences are orthogonal for different users, as their inner products are normally zero. We will consider the Walsh codes in our work. Note that the Walsh codes normally allow a maximum of I orthogonal codes so that one must have $K < I$.

Another multiplexing option is OFDMA, where signals for different users are transmitted over different subcarriers. In this case, the communication pulse in the l-th bit of the k-th user is given by

$$g_{kl}(t) = e^{j2\pi f_k(t - lT_b)}\left[\epsilon(t - lT_b) - \epsilon(t - (l+1)T_b)\right] \tag{6}$$

where $f_k = k\Delta f$, and $\Delta f = \frac{1}{T_b}$ to ensure orthogonality between different users.

In a pure communications system, at the base station, the communications signals of all the L bits for all the K users are effectively added together in the time domain so that the overall transmitted signal over a period of T is given by

$$p(t) = \sum_{k=1}^{K}\sum_{l=0}^{L-1} g_{kl}(t), 0 < t < T. \tag{7}$$

At the communications receivers, the k-th user will receive $p(t)$ in (7) but it will be able to extract its own signal by using either the k-th time slot, spreading code or subcarrier from $p(t)$ due to orthogonality with other users. Then, with perfect time synchronization, the l-th data bit can be decoded using the l-th bit interval of the extracted signal. Thus, the overall communications signal can be represented as a summation of all L bits for all K users in (7).

In a joint radar-communications system, one can use a summation similar to (7) to generate the communications signals at the base station, but the communications signals for different bits and different users within the radar pulse duration can also be linearly combined to generate a radar pulse. Specifically, the communications signals can be linearly combined as

$$s(t) = \sum_{k=1}^{K}\sum_{l=0}^{L-1} c_{kl} g_{kl}(t), 0 < t < T \tag{8}$$

where c_{kl} are the linear weighting coefficients to be determined, with $k = 1, 2, \cdots, K$ and $l = 0, 1, \cdots, L-1$, to approximate the radar pulse $r(t)$. Since the orthogonality and synchronization are not affected by linear combination, the signal in (8) can still be used for information decoding at the communications receivers. The aim of this work is to find the best coefficients of c_{kl} for $s(t)$ that can approximate $r(t)$ as closely as possible. Once this is done, $s(t)$ can be used not only as a radar pulse by the radar receiver but also as information signals by the communications receivers. Define

$$W = \int_0^T |s(t) - r(t)|^2 dt \tag{9}$$

as the mean squared error (MSE) between $s(t)$ in (8) and the radar pulse $r(t)$. The goal is to find the optimum coefficients that minimize W. This will allow the base station to transmit a pulse that overall is a radar pulse for target detection while each component of the pulse delivers information of different data bits for different communications users.

III. Optimization

A. Without constraints

Using (8) in (9), the MSE can be rewritten as

$$W = \int_0^T \left|\sum_{k=1}^{K}\sum_{l=0}^{L-1} c_{kl} g_{kl}(t) - r(t)\right|^2 dt \tag{10}$$

which is a quadratic form of c_{kl}. Denote $\mathbf{c} = [\mathbf{c}_0, \cdots, \mathbf{c}_l, \cdots, \mathbf{c}_{L-1}]$ with $\mathbf{c}_l = [c_{1l}, c_{2l}, \cdots, c_{kl}, \cdots, c_{Kl}]$ for $l = 0, 1, \cdots, L-1$. Also, denote $\mathbf{g}(t) = [\mathbf{g}_0(t), \cdots, \mathbf{g}_l(t), \cdots, \mathbf{g}_{L-1}(t)]^P$ with $\mathbf{g}_l(t) = [g_{1l}(t), g_{2l}(t), \cdots, g_{kl}(t), \cdots, g_{Kl}(t)]^P$, where $(\cdot)^P$ denotes the transpose operation. Then, one has

$$W = \int_0^T |\mathbf{c}\mathbf{g}(t) - r(t)|^2 dt. \tag{11}$$

The above equation can be further expanded as

$$\begin{aligned} W &= \int_0^T \mathbf{c}\mathbf{g}(t)\mathbf{g}(t)^H\mathbf{c}^H dt + \int_0^T |r(t)|^2 dt \\ &\quad - \int_0^T r(t)\mathbf{g}(t)^H dt\mathbf{c}^H - \mathbf{c}\int_0^T \mathbf{g}(t)r^*(t)dt \end{aligned} \tag{12}$$

where $(\cdot)^H$ is the Hermitian operation. Denote $\mathbf{Q} = \int_0^T \mathbf{g}(t)\mathbf{g}(t)^H dt$ and $\mathbf{G} = \int_0^T r(t)\mathbf{g}(t)^H dt$. Then, (12) can be transformed into

$$W = \mathbf{c}\mathbf{Q}\mathbf{c}^H - \mathbf{G}\mathbf{c}^H - \mathbf{c}\mathbf{G}^H + \int_0^T |r(t)|^2 dt. \tag{13}$$

Thus, the minimization of W with respect to $\mathbf{c}$ is a standard quadratic optimization problem, and the optimum coefficient is given by

$$\mathbf{c}^{opt} = \mathbf{G}\mathbf{Q}^{-1}. \tag{14}$$

In this case, the minimum MSE is

$$W_{min} = \int_0^T |r(t)|^2 dt - \mathbf{G}\mathbf{Q}^{-1}\mathbf{G}^H \tag{15}$$

and the optimum pulse to approximate the radar pulse $r(t)$ using communications signals over all bits for all users is given by

$$s^{opt}(t) = \mathbf{G}\mathbf{Q}^{-1}\mathbf{g}(t). \tag{16}$$

This is the general case when the communication signal $g_{kl}(t)$ is not time-limited in each bit interval.

In our work, the communication signal for the l-th bit is time-limited between lT_b and $(l+1)T_b$. For example, the OFDMA signal in (6) is only nonzero between lT_b and $(l+1)T_b$ due to the unit step functions. This is often the case to avoid inter-symbol interference. If the communications signal is time-limited for each bit, one has

$$\int_0^T g_{k'l'}(t) g_{kl}^*(t) dt = 0, \tag{17}$$

when $(\cdot)^*$ is the conjugate operation, and $l \neq l'$ for $k, k' = 1, 2, \cdots, K$, or the communications signals are orthogonal for different bits. It can be verified using (4), (5) and (6) that the TDMA, CDMA and OFDMA signals all satisfy (17). In this case, $\mathbf{Q}$ in (14) becomes a diagonal block matrix, where the $K \times K$ block matrices on the diagonal line are non-zero, while all other block matrices off the diagonal line are zero. Then, one has

$$\mathbf{c}_l^{opt} = \mathbf{G}_l \mathbf{Q}_l^{-1} \tag{18}$$

for $l = 0, 1, \cdots, L-1$, where $\mathbf{Q}_l$ is the l-th $K \times K$ block matrix on the diagonal line of $\mathbf{Q}$ with $\mathbf{Q}_l = \int_{lT_b}^{(l+1)T_b} \mathbf{g}_l(t)\mathbf{g}_l^H(t) dt$ and $\mathbf{G}_l = \int_{lT_b}^{(l+1)T_b} r(t)\mathbf{g}_l(t)^H dt$. The minimum MSE and the optimum pulse can also be simplified as

$$W_{min} = \int_0^T |r(t)|^2 dt - \sum_{l=0}^{L-1} \mathbf{G}_l \mathbf{Q}_l^{-1} \mathbf{G}_l^H \tag{19}$$

and

$$s^{opt}(t) = \sum_{l=0}^{L-1} \mathbf{G}_l \mathbf{Q}_l^{-1} \mathbf{g}_l(t) \tag{20}$$

respectively.

Further, if $g_{kl}(t)$ and $g_{k'l}(t)$ are not only time-limited for each bit, as in (17), but also orthogonal, one has $\int_0^T g_{kl}(t) g_{k'l}^*(t) dt$ for $k \neq k'$ and $l = 0, 1, \cdots, L-1$. The TDMA, CDMA and OFDMA signals all satisfy this. For example, since $\sum_{i=1}^I d_{ki} d_{k'i} = 0$, integrations over the product of any two signals given in (5) give zero for $k \neq k'$. In this case, $\mathbf{Q}_l$ becomes a diagonal matrix with non-zero elements only on the diagonal line as

$$\mathbf{Q}_l = \begin{bmatrix} \int_{lT_b}^{(l+1)T_b} |g_{1l}(t)|^2 dt & \cdots & 0 \\ \vdots & \ddots & \vdots \\ 0 & \cdots & \int_{lT_b}^{(l+1)T_b} |g_{Kl}(t)|^2 dt \end{bmatrix}. \tag{21}$$

Using (21) in (18) - (20), they can be further simplified as

$$c_{kl}^{opt} = \frac{\int_{lT_b}^{(l+1)T_b} r(t) g_{kl}^*(t) dt}{\int_{lT_b}^{(l+1)T_b} |g_{kl}(t)|^2 dt}, \tag{22}$$

$$W_{min} = \int_0^T |r(t)|^2 dt - \sum_{k=1}^K \sum_{l=0}^{L-1} \frac{|\int_{lT_b}^{(l+1)T_b} r(t) g_{kl}^*(t) dt|^2}{\int_{lT_b}^{(l+1)T_b} |g_{kl}(t)|^2 dt} \tag{23}$$

and

$$s^{opt}(t) = \sum_{k=1}^K \sum_{l=0}^{L-1} \frac{g_{kl}(t) \int_{lT_b}^{(l+1)T_b} r(t) g_{kl}^*(t) dt}{\int_{lT_b}^{(l+1)T_b} |g_{kl}(t)|^2 dt}. \tag{24}$$

By substituting the TDMA, CDMA and OFDMA signals in (4) - (6) into (22) - (24), the results for TDMA, CDMA and OFDMA can be obtained. Specifically, for TDMA, one has

$$c_{kl}^{opt} = \frac{K}{T_b} \int_{(l+\frac{k-1}{K})T_b}^{(l+\frac{k}{K})T_b} r(t) dt, \tag{25}$$

$$W_{min} = \int_0^T |r(t)|^2 dt - \frac{K}{T_b} \sum_{k=1}^K \sum_{l=0}^{L-1} |\int_{(l+\frac{k-1}{K})T_b}^{(l+\frac{k}{K})T_b} r(t) dt|^2 \tag{26}$$

and

$$s^{opt}(t) = \frac{K}{T_b} \sum_{k=1}^K \sum_{l=0}^{L-1} \int_{(l+\frac{k-1}{K})T_b}^{(l+\frac{k}{K})T_b} r(t) dt \tag{27}$$
$$[\epsilon\left(t - \left(l + \frac{k-1}{K}\right) T_b\right) - \epsilon\left(t - \left(l + \frac{k}{K}\right) T_b\right)].$$

Similarly, for CDMA, one has

$$c_{kl}^{opt} = \frac{1}{T_b} \sum_{i=1}^I d_{ki} \int_{(l+\frac{i-1}{I})T_b}^{(l+\frac{i}{I})T_b} r(t) dt, \tag{28}$$

$$W_{min} = \int_0^T |r(t)|^2 dt - \frac{1}{T_b} \sum_{k=1}^K \sum_{l=0}^{L-1} |\sum_{i=1}^I d_{ki} \int_{(l+\frac{i-1}{I})T_b}^{(l+\frac{i}{I})T_b} r(t) dt|^2 \tag{29}$$

and

$$s^{opt}(t) = \frac{1}{T_b} \sum_{k=1}^K \sum_{l=0}^{L-1} \sum_{i=1}^I d_{ki} \int_{(l+\frac{i-1}{I})T_b}^{(l+\frac{i}{I})T_b} r(t) dt$$
$$\sum_{i=1}^I d_{ki} \left[\epsilon\left(t - \left(l + \frac{i-1}{I}\right) T_b\right)\right.$$
$$\left. -\epsilon\left(t - \left(l + \frac{i}{I}\right) T_b\right)\right]. \tag{30}$$

For OFDMA, one has

$$c_{kl}^{opt} = \frac{1}{T_b} \int_{lT_b}^{(l+1)T_b} r(t) e^{-j2\pi f_k (t - lT_b)} dt, \tag{31}$$

$$W_{min} = \int_0^T |r(t)|^2 dt - \frac{1}{T_b}\sum_{k=1}^{K}\sum_{l=0}^{L-1} |\int_{lT_b}^{(l+1)T_b} r(t)e^{-j2\pi f_k(t-lT_b)}dt|^2 \quad (32)$$

and

$$s^{opt}(t) = \frac{1}{T_b}\sum_{k=1}^{K}\sum_{l=0}^{L-1}\int_{lT_b}^{(l+1)T_b} r(t)e^{-j2\pi f_k(t-lT_b)}dt \; e^{j2\pi f_k(t-lT_b)}\left[\epsilon(t-lT_b)-\epsilon(t-(l+1)T_b)\right]. \quad (33)$$

One can substitute the radar pulse $r(t)$ given by (1) - (3) in the above equations for further simplification. The accuracy of these optimum coefficients will be examined later.

B. With constraints

In the above subsection, the MSE between $s(t)$ and the radar pulse $r(t)$ is minimized without any constraints on the communications signals. This is suitable for joint radar-communication applications where the radar function is the primary function so that the accuracy of the approximation is of utmost importance. In other applications, the communication function can be the primary function so that the quality of the communications signals cannot be degraded by the linear combination to maintain the same quality of service as the case without linear combination. In this case, constraints on $s(t)$ must be imposed.

The main quality indicator of a communications signal is the signal-to-noise ratio (SNR). For the pure communications system without radar pulse approximation, from (7), the signal of the k-th user is given by $p_k(t) = \sum_{l=0}^{L-1} g_{kl}(t)$ with $0 < t < T$. Thus, the SNR of the k-th user is

$$\gamma_k = \frac{\sum_{l=0}^{L-1}\int_0^T |g_{kl}(t)|^2 dt}{\sigma^2}, \quad (34)$$

where σ^2 is the noise power. For the communications signals discussed before, one has $\int_0^T |g_{kl}(t)|^2 dt = \frac{T_b}{K}$ for TDMA and $\int_0^T |g_{kl}(t)|^2 dt = T_b$ for CDMA and OFDMA. Thus, the SNR becomes $\gamma_k = \frac{LT_b}{K\sigma^2}$ for TDMA and $\gamma_k = \frac{LT_b}{\sigma^2}$ for CDMA and OFDMA. For the joint radar-communication systems, the SNR of the k-th user can be calculated from (8) as

$$\gamma_k = \frac{\sum_{l=0}^{L-1}|c_{kl}|^2\int_0^T |g_{kl}(t)|^2 dt}{\sigma^2}. \quad (35)$$

Thus, they become $\gamma_k = \frac{\sum_{l=0}^{L-1}|c_{kl}|^2 T_b}{K\sigma^2}$ for TDMA and $\gamma_k = \frac{\sum_{l=0}^{L-1}|c_{kl}|^2 T_b}{\sigma^2}$ for CDMA and OFDMA. Thus, to maintain the quality of the communications signals and ensure that the communications signals are not degraded by linear combination, the two SNRs in (34) and (35) should equal to each other to give

$$\sum_{l=0}^{L-1}|c_{kl}|^2 = L, k = 1, 2, \cdots, K \quad (36)$$

for the considered TDMA, CDMA and OFDMA communications signals. The constraint in (36) ensures that the SNR of the communications signal in the joint radar-communication system with linear combination is the same as that in the pure communication system without linear combination so that the linear combination in the dual-functional waveform design does not degrade the communications performance, as it is possible that the linear combination may choose coefficients of c_{kl} that minimizes the MSE but makes (35) smaller than (34) to sacrifice the communications performance for approximation accuracy, if there is no restriction. Equation (36) eliminates this possibility. Thus, this constraint in (36) is used to guarantee that the quality of communications will not be degraded by linear combination, not the successful decoding of communications signals. To guarantee the successful decoding of communications signals, one may impose a pre-defined threshold on (35) or (34) against the noise but this is beyond the scope of the work.

The optimization problem then becomes

$$\min_{\mathbf{c}}\{W\}, s.t. \sum_{l=0}^{L-1}|c_{kl}|^2 = L, k = 1, 2, \cdots, K. \quad (37)$$

This is a quadratic optimization with quadratic constraints problem. From (37), the constraints are not convex, as $\sum_{l=0}^{L-1}|c_{kl}|^2 = L$ is equivalent to $\sum_{l=0}^{L-1}|c_{kl}|^2 \le L$ and $\sum_{l=0}^{L-1}|c_{kl}|^2 \ge L$. Thus, (37) is not convex either [30]. However, solutions may still be found for some special cases. In particular, when all the communications signals are time-limited over each bit, as in (17), $\mathbf{Q}$ becomes a diagonal block matrix such that the MSE can be simplified as

$$W = \sum_{l=0}^{L-1}[\mathbf{c}_l\mathbf{Q}_l\mathbf{c}_l^H - \mathbf{G}_l\mathbf{c}_l^H - \mathbf{c}_l\mathbf{G}_l^H] + \int_0^T |r(t)|^2 dt. \quad (38)$$

Then, using the Lagrange multiplier, the optimization problem in (37) is reformulated as

$$\min_{\mathbf{c},\mu}\{\sum_{l=0}^{L-1}[\mathbf{c}_l\mathbf{Q}_l\mathbf{c}_l^H - \mathbf{G}_l\mathbf{c}_l^H - \mathbf{c}_l\mathbf{G}_l^H] + \sum_{k=1}^{K}\mu_k(\sum_{l=0}^{L-1}|c_{kl}|^2 - L)\} \quad (39)$$

where $\mu = [\mu_1, \cdots, \mu_K]$. The optimization over $\mathbf{c}$ is solved first. Since the last term $\sum_{k=1}^{K}\mu_k L$ does not depend on $\mathbf{c}$, only the first two terms of the objective function in (39) need to be considered for the optimization over $\mathbf{c}$. In this case, since the addition operation is linear, the optimization in (39) is equivalent to the minimization of the l-th term as

$$\min_{\mathbf{c}_l|\mu}\{\mathbf{c}_l\mathbf{Q}_l\mathbf{c}_l^H - \mathbf{G}_l\mathbf{c}_l^H - \mathbf{c}_l\mathbf{G}_l^H + \sum_{k=1}^{K}\mu_k|c_{kl}|^2\} \quad (40)$$

where $\cdot|\mu$ means the optimization given fixed values of μ. Denote $\mathbf{\Lambda} = \begin{bmatrix} \mu_1 & \cdots & 0 \\ \vdots & \ddots & \vdots \\ 0 & \cdots & \mu_K \end{bmatrix}$. The optimization in (40) becomes

$$\min_{\mathbf{c}_l|\mu}\{\mathbf{c}_l\left[\mathbf{Q}_l + \mathbf{\Lambda}\right]\mathbf{c}_l^H - \mathbf{G}_l\mathbf{c}_l^H - \mathbf{c}_l\mathbf{G}_l^H\} \quad (41)$$

which is a standard quadratic optimization problem with optimum coefficients satisfying

$$\mathbf{c}_l^{opt} = \mathbf{G}_l\left[\mathbf{Q}_l + \mathbf{\Lambda}\right]^{-1}. \quad (42)$$

This is not a final solution due to the dependence of the optimum coefficients on the unknown Lagrange multipliers μ. However, when the communications signals are also orthogonal for different users, $\mathbf{Q}_l$ becomes a diagonal matrix too as in (21). In this case, from (42), the optimum coefficient can be calculated as

$$c_{kl}^{opt} = \frac{\int_{lT_b}^{(l+1)T_b} r(t) g_{kl}^*(t) dt}{\mu_k + \int_{lT_b}^{(l+1)T_b} |g_{kl}(t)|^2 dt} \tag{43}$$

for $k = 1, 2, \cdots, K$ and $l = 0, 1, \cdots, L-1$. Further, one can substitute the optimum $\mathbf{c}$ given by (42) into (39) to have

$$\min_{\mu} \{ - \sum_{l=0}^{L-1} \mathbf{G}_l \left[\mathbf{Q}_l + \mathbf{\Lambda} \right]^{-1} \mathbf{G}_l^H - L \sum_{k=1}^{K} \mu_k \} \tag{44}$$

which is an optimization over μ only now. When the communications signals are orthogonal for different users, this can be rewritten as

$$\min_{\mu} \{ - \sum_{l=0}^{L-1} \sum_{k=1}^{K} \frac{| \int_{lT_b}^{(l+1)T_b} r(t) g_{kl}^*(t) dt|^2}{\mu_k + \int_{lT_b}^{(l+1)T_b} |g_{kl}(t)|^2 dt} - L \sum_{k=1}^{K} \mu_k \}. \tag{45}$$

One sees that each μ_k can be optimized separately. By taking the first-order derivative of the k-th term in the objective function in (45) with respect to μ_k, letting the derivative be zero and solving the equation for μ_k, one can obtain

$$\sum_{l=0}^{L-1} \left| \frac{\int_{lT_b}^{(l+1)T_b} r(t) g_{kl}^*(t) dt}{\mu_k + \int_{lT_b}^{(l+1)T_b} |g_{kl}(t)|^2 dt} \right|^2 = L \tag{46}$$

for $k = 1, \cdots, K$, which can be solved to find the k-th Lagrange multiplier. Alternatively, one can use the constraint on the SNR in (36) directly to find (45). They are equivalent. Denote the solution to (46) as μ_k^{opt}. The optimum coefficient is then calculated as

$$c_{kl}^{opt} = \frac{\int_{lT_b}^{(l+1)T_b} r(t) g_{kl}^*(t) dt}{\mu_k^{opt} + \int_{lT_b}^{(l+1)T_b} |g_{kl}(t)|^2 dt} \tag{47}$$

for $k = 1, 2, \cdots, K$ and $l = 0, 1, \cdots, L-1$, where μ_k has been replaced by μ_k^{opt}.

For the TDMA signal, $\int_{lT_b}^{(l+1)T_b} |g_{kl}(t)|^2 dt = \frac{T_b}{K}$. For the CDMA and OFDMA signals, $\int_{lT_b}^{(l+1)T_b} |g_{kl}(t)|^2 dt = T_b$. All of them are constants independent of l. Using this fact in (46), the equation can be solved for μ_k and the solution is then used in (47) to give

$$c_{kl}^{opt} = \frac{\int_{lT_b}^{(l+1)T_b} r(t) g_{kl}^*(t) dt}{\sqrt{\frac{1}{L} \sum_{l=0}^{L-1} \left| \int_{lT_b}^{(l+1)T_b} r(t) g_{kl}^*(t) dt \right|^2}} \tag{48}$$

for $k = 1, 2, \cdots, K$ and $l = 0, 1, \cdots, L-1$. Then using (48) in W, the minimum MSE can be calculated as

$$W_{min} = \int_0^T |r(t)|^2 dt + \sum_{l=0}^{L-1} \sum_{k=1}^{K} \frac{| \int_{lT_b}^{(l+1)t_b} r(t) g_{kl}^*(t) dt|^2}{\sqrt{\frac{1}{L} \sum_{l=0}^{L-1} \left| \int_{lT_b}^{(l+1)T_b} r(t) g_{kl}^*(t) dt \right|^2}} \left[\frac{\int_{lT_b}^{(l+1)T_b} |g_{kl}(t)|^2 dt}{\sqrt{\frac{1}{L} \sum_{l=0}^{L-1} \left| \int_{lT_b}^{(l+1)T_b} r(t) g_{kl}^*(t) dt \right|^2}} - 2 \right]. \tag{49}$$

The optimum pulse is obtained by using (48) in (8) to give

$$s^{opt}(t) = \sum_{k=1}^{K} \sum_{l=0}^{L-1} \frac{g_{kl}(t) \int_{lT_b}^{(l+1)T_b} r(t) g_{kl}^*(t) dt}{\sqrt{\frac{1}{L} \sum_{l=0}^{L-1} \left| \int_{lT_b}^{(l+1)T_b} r(t) g_{kl}^*(t) dt \right|^2}}, \quad 0 < t < T. \tag{50}$$

Comparing (50) with (24), one sees that the calculation of the approximate pulse in (24) without SNR constraint requires $2KL$ multiplications, KL divisions, KL squaring, $2KL$ integrations and KL additions, while the calculation of the approximate pulse in (50) with SNR constraint requires $2KL$ multiplications, $KL+1$ divisions, KL squaring, KL integrations and KL^2 additions, and KL square rooting, for each time instant. The computational complexity is proportional to K and L. For compactness, the optimum values for TDMA, CDMA and OFDMA are not given there but they can be easily obtained by replacing $g_{kl}(t)$ in (48) - (50) with the relevant signals given in (4) - (6).

Comparing the optimum coefficients for the unconstrained case in (22) with the optimum coefficients for the constrained case in (48), one sees that the constraint on the SNR in (36) leads to the denominator in (48). This constraint is essentially a normalization operation over the coefficients given in (22) for the unconstrained case, in order to satisfy the SNR constraint in (36) while minimize the MSE. In the next section, numerical examples will be given to show the accuracy of using (8) to approximate $r(t)$ at the base station.

IV. Numerical Results and Discussion

In this section, numerical examples are presented to show the accuracy of the proposed approximation to radar pulses. Three commonly used radar pulses are examined, the LFM pulse in (1), the Gaussian pulse in (2) and the Barker sequence in (3). For the Barker sequence, the Barker-13 sequence is used, where $M = 13$ and $\mathbf{b} = [+1, +1, +1, +1, +1, -1, -1, +1, +1, -1, +1, -1, +1]$ for different b_m. The bandwidth of the radar waveform is set to 1 MHz with a time-bandwidth product of 100 so that the radar pulse duration is $T = 10^{-4}$ seconds. Also, three different types of communications signals are used, the TDMA signal in (4) that achieves user orthogonality in the time domain, the CDMA signal in (5) that achieves user orthogonality in the code domain, and the OFDMA signal in (6) that achieves user orthogonality in the frequency domain. The processing gain of CDMA is set to $I = 8$. In the following figures, the title of

This article has been accepted for publication in a future issue of this journal, but has not been fully edited. Content may change prior to final publication. Citation information: DOI 10.1109/TCOMM.2020.2994215, IEEE Transactions on Communications

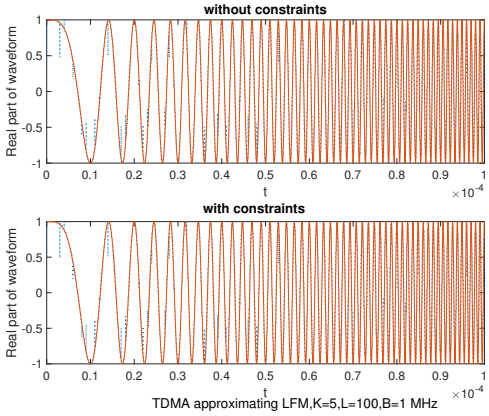

Fig. 1. Comparison of the exact radar LFM pulse (solid line) and the approximated LFM pulse (dotted line) using the TDMA signals.

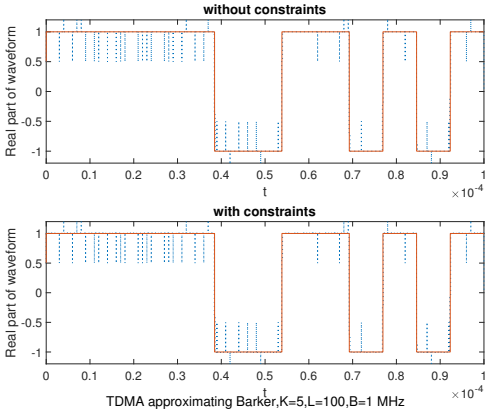

Fig. 3. Comparison of the exact radar Barker-13 pulse (solid line) and the approximated Barker-13 pulse (dotted line) using the TDMA signals.

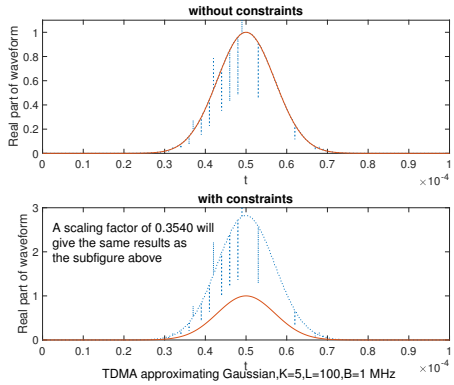

Fig. 2. Comparison of the exact radar Gaussian pulse (solid line) and the approximated Gaussian pulse (dotted line) using the TDMA signals.

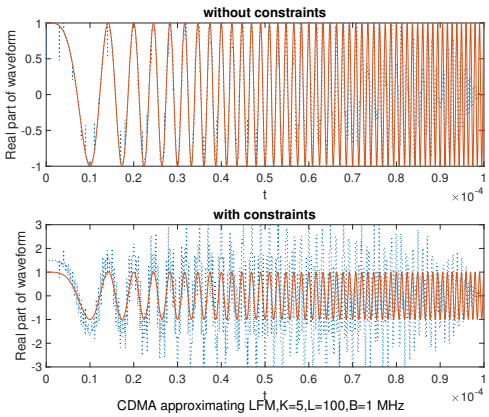

Fig. 4. Comparison of the exact radar LFM pulse (solid line) and the approximated LFM pulse (dotted line) using the CDMA signals.

"without constraints" refers to curves obtained by using (24), while the title "with constraints" refers to curves obtained by using (50).

Figs.1 - 3 compare the exact radar pulses with the approximate radar pulses for LFM, Gaussian and Barker, respectively, using the TDMA signals. The upper part of each figure uses the optimization without SNR constraint, while the lower part of each figure uses the optimization with SNR constraint. In these figures, $K = 5$ and $L = 100$. Two observations can be made. Firstly, the optimization without constraint derived in Section III.A generates very accurate approximation to the exact radar pulse in all three cases. In fact, there is almost a perfect match between the solid lines and the dotted lines, except at a few time instants where the dotted lines are spiky. The dotted lines are spiky at these time instants because the values of the real part of the waveform at these time instants are significantly larger or smaller than their neighboring values, not because there are many different values for the same time instant. For example, in the upper part of Fig. 2, the real part of the waveform equals to 0.4542 when $t = 0.53 \times 10^{-4}$, while its neighboring values equal to 0.9193 and 0.9083, leading to the spike. These spikes may be reduced or eliminated by performing smoothing after combining. Thus, the combined communications signals can be well used to generate different radar pulses for radar functions. Secondly, the optimization with SNR constraint derived in Section III.B has similar accuracy to that without constraint for the LFM and Barker pulses, but not the Gaussian pulse. Although the approximated pulse is still Gaussian, as can be seen from Fig. 2, there is considerable mismatch between them. Interestingly, it is found that the approximated Gaussian pulse and the exact Gaussian pulse has a fixed ratio of 2.8, which means that the Gaussian radar pulse can still be accurately generated even with the SNR constraint by first using (50) and then a scaling of 0.36.

Figs. 4 - 6 compare the exact radar pulse with the approximated pulse using the CDMA signals. Again, the upper part refers to optimization without constraint, while the lower part refers to optimization with constraint, when $K = 5$ and $L = 100$. For the optimization without constraint in the upper parts of these figures, there is almost perfect match between the exact pulse and the approximated pulse other than a few spiky time instants, very similar to the TDMA signals. For the optimization with SNR constraint in the lower parts of these figures, the approximated LFM pulse can still track the trend of the exact LFM pulse but its values are too large in general, the approximated Barker pulse has very good match with the exact Barker pulse in the flat areas but very spiky in

This article has been accepted for publication in a future issue of this journal, but has not been fully edited. Content may change prior to final publication. Citation information: DOI 10.1109/TCOMM.2020.2994215, IEEE Transactions on Communications

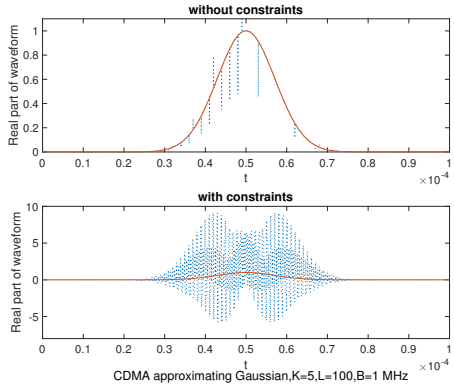

Fig. 5. Comparison of the exact radar Gaussian pulse (solid line) and the approximated Gaussian pulse (dotted line) using the CDMA signals.

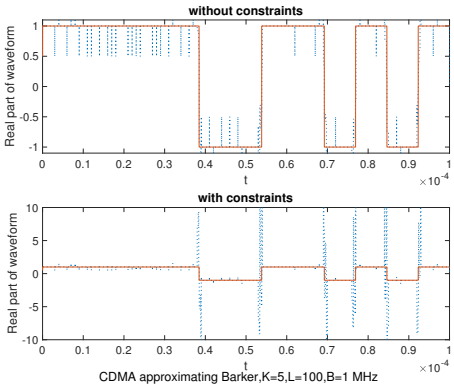

Fig. 6. Comparison of the exact radar Barker-13 pulse (solid line) and the approximated Barker-13 pulse (dotted line) using the CDMA signals.

the transitional areas, while the approximated Gaussian pulse becomes a mixture of Gaussian functions and is very far away from the exact Gaussian pulse.

Fig. 7 compares the exact radar pulse with the approximate radar pulse using the OFDMA signals without SNR constraint. From the figure, the LFM pulse can be well approximated, the Gaussian pulse can be perfectly approximated even without any spiky time instants, while the Barker pulse cannot be approximated at all, as the approximated pulse is always 1. For the optimization with SNR constraint, the results are even worse than CDMA. They are not shown here to save space. In general, the accuracy of the radar pulse using the OFDMA signals is lower than TDMA and CDMA, although OFDMA is a very popular technology in several cellular and Wi-Fi standards. This may be caused by the fact that TDMA and CDMA achieve the orthogonality using time resource blocks while OFDMA achieves the orthogonality using frequency resource blocks. In our work, different bits in the time domain are used to generate the radar pulse. Thus, time orthogonality is more advantageous than frequency orthogonality. In particular, TDMA has a fine time resolution of $\frac{T_b}{K}$ for different users. To increase the accuracy of OFDMA, different subcarriers in the frequency domain may be used to generate the radar spectrum instead. However, this will be more difficult than the time domain method, as the radar spectrum is more

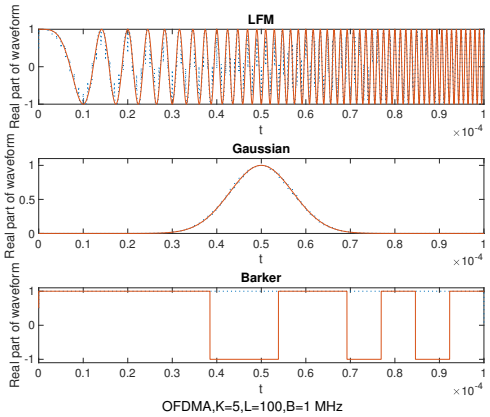

Fig. 7. Comparison of the exact radar pulse (solid line) and the approximate pulse (dotted line) using the OFDMA signals without SNR constraint.

complicated than the radar pulse for optimization. Due to the length restriction, this will be investigated in the future.

Note that the approximated Gaussian pulse with SNR constraint has low accuracy in Figs. 2 and 5. This can be explained as follows. The approximated pulse without SNR constraint is given by (24), while the approximated pulse with SNR constraint is given by (50). Their only difference is the denominator where (24) has

$$\int_{lT_b}^{(l+1)T_b} |g_{kl}(t)|^2 dt \tag{51}$$

while (50) has

$$\sqrt{\frac{1}{L}\sum_{l=0}^{L-1}\left|\int_{lT_b}^{(l+1)T_b} r(t)g_{kl}^*(t)dt\right|^2}. \tag{52}$$

Since the Gaussian pulse without SNR constraint has high accuracy in Figs. 2 and 5, the low accuracy with SNR constraint must be caused by the different denominator. Using the Schwartz inequality, one has

$$\left|\int_{lT_b}^{(l+1)T_b} r(t)g_{kl}^*(t)dt\right|^2 \leq \int_{lT_b}^{(l+1)T_b} |r(t)|^2 dt \int_{lT_b}^{(l+1)T_b} |g_{kl}^*(t)|^2 dt. \tag{53}$$

For LFM and Barker pulses, they have constant amplitudes so that $\int_{lT_b}^{(l+1)T_b} |r(t)|^2 dt = T_b$ from (1) and (3). However, for the Gaussian pulse, $\int_{lT_b}^{(l+1)T_b} |r(t)|^2 dt < T_b$ as $r(t) < 1$ from (2). This makes the denominator in (50) much smaller than the denominator in (24) for the Gaussian pulse, or the approximated pulse in (50) much larger than that in (24). Indeed, from Figs. 2 and 5, the approximated Gaussian pulse with SNR constraint is always larger than the exact pulse or the approximated Gaussian pulse without SNR constraint. In general, radar detection prefers constant modulus pulse to non-constant modulus pulse.

Figs. 8 and 9 compare the magnitude of the normalized ambiguity functions of the pulses approximated using TDMA, CDMA and OFDMA without and with SNR constraint, respectively. For the case without SNR constraint in Fig. 8,

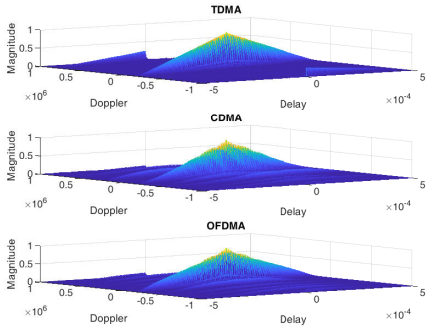

Fig. 8. Comparison of the magnitude of the normalized ambiguity functions of the approximated LFM pulses using TDMA, CDMA and OFDMA without SNR constraint.

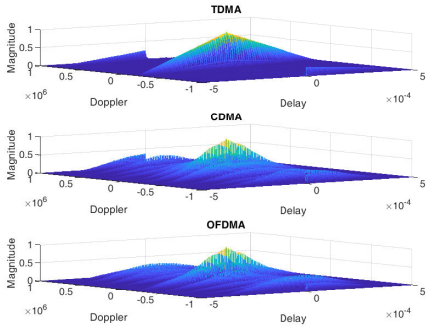

Fig. 9. Comparison of the magnitude of the normalized ambiguity functions of the approximated LFM pulses using TDMA, CDMA and OFDMA with SNR constraint.

the ambiguity functions for TDMA, CDMA and OFDMA are almost identical and can be shown to be similar to that of the exact pulse. This agrees with observations from Figs. 1, 4 and 7. For the case with SNR constraint in Fig. 9, the ambiguity function of TDMA is the same as the case without SNR constraint, which can also be seen from Fig. 1. The ambiguity functions of CDMA and OFDMA have bigger gaps between peaks for different delays, although the overall shape is still the same as the case without SNR constraint.

Figs. 10 - 12 show the effects of different system parameters on the accuracy of the generated radar pulses for the MSE minimization without SNR constraint. The accuracy is represented by the normalized minimum MSE, which is obtained by normalizing the minimum MSE given in (26), (29) and (32) with the radar pulse energy of $\int_0^T |r(t)|dt$. The result for Barker pulse is not given in Fig. 12 as its MSE is too large to be shown.

From Fig. 10, one sees that the normalized minimum MSE decreases when L increases. This is expected. When L increases, for a fixed radar pulse duration T, the bit interval decreases as $T_b = \frac{T}{L}$. This reduces the time slot of $\frac{T_b}{K}$ within each bit allocated to different communications users too, making its time resolution finer when considering the orthogonal time functions in (4) as an orthonormal basis that decomposes $r(t)$. Hence, the accuracy of generated radar pulse

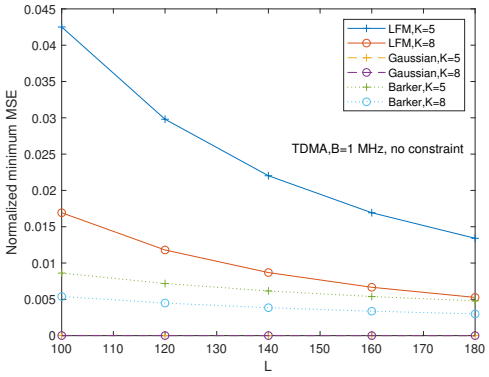

Fig. 10. The normalized minimum MSE for TDMA signals.

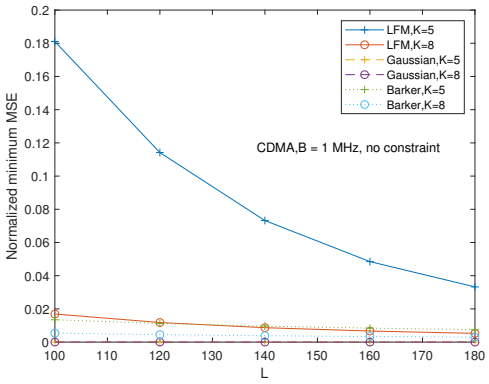

Fig. 11. The normalized minimum MSE for CDMA signals.

increases. Also, the accuracy of the generated radar pulse improves when K increases too for the same reason, as the time slot of $\frac{T_b}{K}$ for each user decreases when K increases to make the orthogonal basis functions finer. Finally, the Gaussian pulse has the smallest normalized MSE, followed by the Barker pulse and the LFM pulse. However, all of them have a normalized minimum MSE of less than 4.5%, showing how accurately the radar pulse generated using TDMA signals is.

Similar observations can be made for the CDMA signals in Fig. 11. Again, the MSE decreases with K and L. The value of K can be considered as the degree of freedom in the

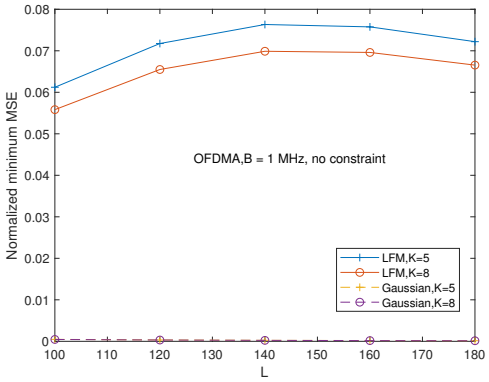

Fig. 12. The normalized minimum MSE for OFDMA signals.

user dimension, while the value of L can be considered as the degree of freedom in the bit dimension. In this case, most normalized MSEs are less than 2%, except the LFM pulse with five users.

Both TDMA and CDMA signals achieve the orthogonality using either time slots or chips as time resource blocks, while the OFDMA signal achieves the orthogonality using frequency resource blocks. Indeed, from Fig. 12, the MSE first increases then decreases when L increases, unlike Figs. 10 and 11. The largest MSE is achieved when L is around 140, which should be avoided. This can be explained as follows. When L increases, the bit interval T_b decreases, because $T_b = \frac{T}{L}$ and $T = 10^{-4}$ seconds is fixed in the simulation. Since the linear combination is performed over different bits, the decrease of T_b means the time resolution increases or the time interval becomes finer to approximate $r(t)$. This reduces the MSE. On the other hand, when L increases, the frequency separation $\Delta f = \frac{1}{T_b} = \frac{L}{T}$ increases for a fixed T. The increase of Δf means the frequency resolution decreases or the frequency interval becomes more coarse to approximate $r(t)$. This increases the MSE. The overall MSE is determined by these two counteracting factors. When L is small, the frequency resolution must be dominant so that the MSE increases with L. When L is large, the time resolution must be dominant so that the MSE decreases with L. The normalized MSE is less than 8% in all cases.

Also, from Figs. 1 - 7, the optimization without SNR constraint can almost perfectly generate all the radar pulses using any of the communications signals considered. This is the case when the radar function is the primary function in the joint radar-communication system, while the communications function is only a secondary use of the joint system so that the accuracy is of priority. When the communications function is the primary function of the joint radar-communication system such that SNR constraint on the communications signal is imposed, the TDMA signal is the best option to approximate all three radar pulses, while the CDMA signal only works for the Barker pulse and the OFDMA signal does not work at all. However, the optimization with SNR constraint only differs from the optimization without SNR constraint by a scaling factor, as explained below.

Comparing the optimum coefficients in (22) with those in (48), one notices that (48) is actually a scaled version of (22) with a scaling factor of

$$Q_k = \sqrt{\frac{1}{L}\sum_{l=0}^{L-1}\left|\frac{\int_{lT_b}^{(l+1)T_b} r(t) g_{kl}^*(t)dt}{\int_{lT_b}^{(l+1)T_b}|g_{kl}(t)|^2 dt}\right|^2}. \tag{54}$$

The scaling factor Q_k depends on the user index k but is independent of the bit index l. Hence, it is constant for different bits of the same user. Thus, in the optimization with constraint, if one increases the amplitude of the communications signals for the k-th user in (4) - (6) from 1 to Q_k, $g_{kl}(t)$ will be replaced by $Q_k g_{kl}(t)$ in Q_k so that the scaling factor now becomes

$$\sqrt{\frac{1}{L}\sum_{l=0}^{L-1}\left|\frac{\int_{lT_b}^{(l+1)T_b} r(t) Q_k g_{kl}^*(t)dt}{\int_{lT_b}^{(l+1)T_b}|Q_k g_{kl}(t)|^2 dt}\right|^2} = 1. \tag{55}$$

In this case, the optimum coefficients in the constrained case become the same as those in (22) in the unconstrained case. This suggests that the optimization with SNR constraint can still achieve the same approximation accuracy as the optimization without SNR constraint by first increasing the transmission power from 1 to Q_k^2 for the k-th user and then combining the communications signals at the transmitter, at the cost of higher transmission power than the unconstrained case.

Finally, the above results consider the waveforms of the communications users only. In practice, the data symbols of the communications users will occur. In this case, the communications signal in (7) becomes

$$p(t) = \sum_{k=1}^{K}\sum_{l=0}^{L-1} s_{kl} g_{kl}(t) \tag{56}$$

where s_{kl} is the l-th symbol of the k-th user. Using this signal in the optimization, the optimum coefficient and the approximated pulse without SNR constraint become

$$c_{kl}^{opt} = \frac{\int_{lT_b}^{(l+1)T_b} r(t) s_{kl}^* g_{kl}^*(t)dt}{\int_{lT_b}^{(l+1)T_b}|s_{kl}|^2|g_{kl}(t)|^2 dt}, \tag{57}$$

and

$$s^{opt}(t) = \sum_{k=1}^{K}\sum_{l=0}^{L-1}\frac{g_{kl}(t)\int_{lT_b}^{(l+1)T_b} r(t) g_{kl}^*(t)dt}{\int_{lT_b}^{(l+1)T_b}|g_{kl}(t)|^2 dt} \tag{58}$$

respectively, and those with SNR constraint become

$$c_{kl}^{opt} = \frac{\int_{lT_b}^{(l+1)T_b} r(t) s_{kl}^* g_{kl}^*(t)dt}{\sqrt{\frac{1}{L}\sum_{l=0}^{L-1}\left|\int_{lT_b}^{(l+1)T_b} r(t) s_{kl}^* g_{kl}^*(t)dt\right|^2}} \tag{59}$$

and

$$s^{opt}(t) = \sum_{k=1}^{K}\sum_{l=0}^{L-1}\frac{g_{kl}(t)\int_{lT_b}^{(l+1)T_b} r(t) g_{kl}^*(t)dt}{\sqrt{\frac{1}{L}\sum_{l=0}^{L-1}\left|\int_{lT_b}^{(l+1)T_b} r(t) g_{kl}^*(t)dt\right|^2}} \tag{60}$$

respectively, where s_{kl} occurred as $|s_{kl}|^2$ in $s^{opt}(t)$ but has been cancelled out from the fraction. Three observations can be made.

Firstly, the optimum coefficients c_{kl} in (57) and (59) become dependent of the symbols s_{kl}, when the symbols of the communications users are considered. This is not an issue, because the base station has knowledge of all symbols to calculate the optimum coefficients.

Secondly, the approximate pulses in (58) and (60) become independent of the symbols s_{kl}. This might be an issue for data transmission, as the communications receiver has no data symbols to decode, if $s^{opt}(t)$ in (58) or (60) is transmitted. However, for pilots and reference signals, this may not be

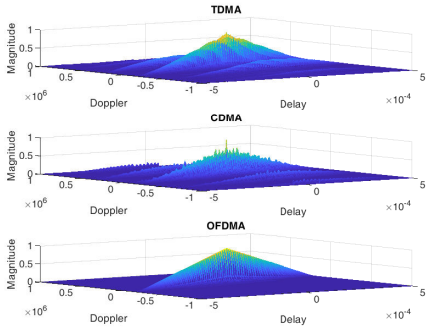

Fig. 13. The ambiguity functions using TDMA, CDMA, OFDMA when $K = 100$ and $L = 2$ for $B = 1MHz$.

an issue because they do not need decoding. For example, in the fourth generation networks, the synchronization often uses known Zadoff-Chu or m-sequences. The base station can choose communications users with the same pilot bits to approximate the pulse in the linear combination. Fig. 13 shows the ambiguity functions of the approximate LFM pulses from TDMA, CDMA and OFDMA when $K = 100$ and $L = 2$ without SNR constraint in (58). One sees that, with as few as two pilot bits of the same value, good approximate pulses can be obtained. The transmitted pulse can be then obtained by scaling (58) and (60) with the pilot value, as scaling does not change the correlation property of the ambiguity function.

Finally, if one has to use the data symbols to approximate the radar pulse, one can use the coefficients in (22) and (48) by ignoring the data symbols of the communications users, but can combine the signal for transmission and approximation as

$$s(t) = \sum_{k=1}^{K}\sum_{l=0}^{L-1} \frac{s_{kl} g_{kl}(t) \int_{lT_b}^{(l+1)T_b} r(t) g_{kl}^*(t) dt}{\int_{lT_b}^{(l+1)T_b} |g_{kl}(t)|^2 dt} \tag{61}$$

in the case without SNR constraint, and

$$s(t) = \sum_{k=1}^{K}\sum_{l=0}^{L-1} \frac{s_{kl} g_{kl}(t) \int_{lT_b}^{(l+1)T_b} r(t) g_{kl}^*(t) dt}{\sqrt{\frac{1}{L}\sum_{l=0}^{L-1} \left| \int_{lT_b}^{(l+1)T_b} r(t) g_{kl}^*(t) dt \right|^2}} \tag{62}$$

in the case with SNR constraint, to have the data symbols for decoding at the communications receivers, as s_{kl} only occurs once in the overall signal, not in the linear coefficients. The pulses in (61) and (62) are not optimum any more, due to the randomness of the data symbols s_{kl}. They are not even LFM, Gaussian or Barker pulses. However, they have similar ambiguity functions to the approximated LFM, Gaussian or Barker pulses in (58) and (60). To see this, the ambiguity function is defined as

$$\chi(\tau, f) = \int_{-\infty}^{\infty} s(t) s^*(t-\tau) e^{j2\pi f t} dt \tag{63}$$

where f is the Doppler frequency and τ is the delay. Using (61) or (62)in this definition, due to the orthogonality of users and bits, one sees that s_{kl} from $s(t)$ will be multiplied with s_{kl}^* from $s^*(t-\tau)$ to become $|s_{kl}|^2$, which is a constant for constant modulus modulation schemes. Thus, for data symbols with constant modulus, (61) and (62) can still be used for target detection. They have the same ambiguity functions scaled by $|s_{kl}|^2$ as those of (58) and (60) but they do not approximate the original LFM, Gaussian or Barker pulses.

In summary, the proposed methods can be used for both pilot and information signals. For pilot signals, the approximated pulses need to be scaled by the pilot value. For information signals, the approximated pulse is not optimum any more due to the randomness of information but they still have the same ambiguity functions as those without considering the communications symbols.

V. Conclusion

In this paper, the problem of dual-functional waveform design for joint radar-communication systems has been studied. A new method that combines the signals from multiple communications users in different bit intervals has been proposed to generate the radar waveform. The accuracy of the generated radar pulse has been examined for both optimization with SNR constraint and optimization without SNR constraint. Numerical results have been presented to show that the optimization without SNR constraint can generate very accurate radar pulses in almost all the cases considered, while the optimization with SNR constraint requires scaling before combination. They have also showed that the TDMA signal is the best option for generation, and that the Gaussian pulse is the easiest radar pulse to generate. The approximation error can be further reduced by increasing the number of communications users or the number of data bits in the combination. Future works include the extension of our work to multi-antenna systems by exploring the additional degree of freedom in the space domain.

References

[1] B. Paul, A.R. Chiriyath, D.W. Bliss, "Survey of RF communications and sensing convergence research," *IEEE Access*, vol. 5, pp. 252 - 270, Feb. 2017.

[2] J.M. Chapin and W.H. Lehr, "Cognitive radios for dynamic spectrum access - The path to market success for dynamic spectrum access technology," *IEEE Commun. Mag.*, vol. 45, pp. 96 - 103, May 2007.

[3] Y. Li, L. Zheng, M. Lops, X. Wang, "Interference removal for radar/communication co-existence: the random scattering case," *IEEE Trans. Wireless Commun.*, vol. 18, pp. 4831 - 4845, Oct. 2019.

[4] S. Tsugawa, "Energy ITS: Another application of vehicular communications," *IEEE Commun. Mag.*, vol. 48, pp. 120 - 126, Nov. 2010.

[5] S. Kay, *Fundamentals of Statistical Signal Processing: Estimation Theory*, Prentice Hall: New York, NY, 1993.

[6] C. Sturm and W. Wiesbeck, "Waveform design and signal processing aspects for fusion of wireless communications and radar sensing," *Proc. IEEE*, vol. 99, pp. 1236-1259, Jul. 2011.

[7] S.H. Dokhanchi, B.S. Mysore, K.V. Mishra, B. Ottersten, "A mmWave automotive joint radar-communications system," *IEEE Trans. Aerospace and Electronic Sys.*, vol. 55, pp. 1241 - 1260, June 2019.

[8] S. D. Blunt, P. Yatham, and J. Stiles, "Intrapulse radar-embedded communications," *IEEE Trans. Aerosp. Electron. Syst.*, vol. 46, pp. 1185 1200, Jul. 2010.

[9] N. Decarli, F. Guidi, and D. Dardari, "A novel joint RFID and radar sensor network for passive localization: design and performance bounds," *IEEE J. Sel. Topics Signal Process.*, vol. 8, pp. 80 - 95, Feb. 2014.

[10] Z. Geng, R. Xu, H. Deng, B. Himed, "Fusion of radar sensing and wireless communications by embedding communication signals into the radar transmit waveform," *IET Radar, Sonar & Navigation*, vol. 12, pp. 632 - 640, 2018.

[11] S.Y. Nusenu, W.-Q. Wang, and A. Basit, "Time-modulated FD-MIMO array for integrated radar and communication systems," *IEEE Wireless and Propagation Lett.*, vol. 17, pp. 1015 - 1019, June 2018.

[12] M.J. Nowak, M. Wicks, Z. Zhang, Z. Wu, "Co-designed radar-communication using linear frequency modulation waveform," *IEEE Aerospace and Electronic Systems Mag.*, vol. 31, pp. 28 - 35, Oct. 2016.

[13] M.J. Nowak, Z. Zhang, L. LoMonte, M. Wicks, Z. Wu, "Mixed-modulated linear frequency modulated radar-communications," *IET Radar, Sonar & Navigation*, vol. 11, pp. 313 - 320, 2017.

[14] S.D. Blunt, J.G. Metcalf, C.R. Biggs, and E. Perrins, "Performance characteristics and metrics for intra-pulse radar-embedded communication," *IEEE J. Select. Areas Commun.*, vol. 29, pp. 2057 - 2066, Dec. 2011.

[15] A. Ahmed, Y.D. Zhang, and B. Himed, "Multi-user dual-function radar-communications exploiting sidelobe control and waveform diversity," *Proc. 2018 IEEE Radar Conference*, Oklahoma City, US, 23-27 April 2018.

[16] A. Hassanien, M.G. Amin, Y.D. Zhang, and F. Ahmad, "Dual-function radar-communications: information embedding using sidelobe control and waveform diversity,"' *IEEE Trans. Signal Processing*, vol. 64, pp. 2168 - 2181, Apr. 2016.

[17] Y. Zhang, Q. Li, L. Huang and J. Song, "Waveform design for joint radar-communication system with multi-user based on MIMO radar," *Proc. 2017 IEEE Radar Conference*, Seattle, US, 8-12 May 2017.

[18] Q. Zhang, Y. Zhou, L. Zhang, Y. Gu, J. Zhang, "Waveform design for a dual-function radar-communication system based on CE-OFDM-PM signal," *IET Radar, Sonar & Navigation*, vol. 13, pp. 566 - 572, 2019.

[19] C. Sturm, T. Zwick, and W. Wiesbeck, "An OFDM system concept for joint radar and communications operations," *Proc. 2009 IEEE Vehicular Technol. Conf. Spring*, Barcelona, Spain, 26 - 29 April 2009.

[20] A. Aubry, A. De Maio, M. Piezzo, A. Farina, "Radar waveform design in a spectrally crowded environment via nonconvex quadratic optimization," *IEEE Trans. Aerospace and Electronic Systems*, vol. 50, pp. 1138 - 1152, Apr. 2014.

[21] V. Karimi, R. Mohseni, S. Samadi, "Adaptive OFDM waveform design for cognitive radar in signal-dependent clutter," *IEEE Systems Journal*, 2019.

[22] V. Karimi, R. Mohseni, M.R. Khosravi, "An edge computing framework based on OFDM radar for low grazing angle target tracking," *EURASIP J. Wireless Com. Network*, vol. 18, 2020.

[23] A. Hassanien, M.G. Amin, Y.D. Zhang, F. Ahmad, "Signaling strategies for dual-function radar communications: an overview," *IEEE A&E Systems Mag.*, vol. 31, pp. 36 - 45, Oct. 2016.

[24] F. Liu, L. Zhou, C. Masouros, A. Li, W. Luo, A. Petropulu, "Toward dual-functional radar-communication systems: optimal waveform design," *IEEE Trans. Signal Processing*, vol. 66, pp. 4264 - 4279, Aug. 2018.

[25] F. Liu, C.. Masouros, A. Li, H. Sun, L. Hanzo, "MU-MIMO communications with MIMO radar: from co-existence to joint transmission," *IEEE Trans. Wireless Commun., vol. 17, pp. 2755 - 2770, Apr. 2018.*

[26] S. Shi, Z. Wang, Z. He, Z. Cheng, "Constrained waveform design for dual-functional MIMO radar-communication system," *Signal Processing*, vol. 171, June 2020.

[27] B.R. Mahafza, *Introduction to Radar Analysis*, 2nd Ed. CRC Press: New York, NY. 2017.

[28] J.D. Taylor (Ed.), *Ultrawideband Radar Applications and Design*, CRC Press: New York, NY. 2012.

[29] M.I. Skolnik, *Introduction to Radar Systems*, 3rd Ed. McGrawHill: New York, NY, 2001.

[30] S. Boyd and L. Vandenberghe, *Convex Optimization*, Cambridge University Press: Cambridge, UK. 2004.